Nanoscale piezoelectric response of ZnO nanowires measured using a nanoindentation technique

Esteban Broitman, Muhammad Yousuf Soomro, Jun Lu, Magnus Willander and Lars Hultman

Original Publication:

Esteban Broitman, Muhammad Yousuf Soomro, Jun Lu, Magnus Willander and Lars Hultman, Nanoscale piezoelectric response of ZnO nanowires measured using a nanoindentation technique, 2013, Physical Chemistry, Chemical Physics - PCCP, (15), 26, 11113-11118.
http://dx.doi.org/10.1039/c3cp50915j

Nanoscale Piezoelectric Response of ZnO Nanowires by a Nanoindentation Technique

E.Broitman[1,*], Muhammad Yousuf Soomro[2], Jun Lu[1],

Magnus Willander[2], and Lars Hultman[1]

[1] *Thin Film Physics Division, IFM, Linköping University, SE-581-83 Linköping, Sweden.*

[2] *ITN, Campus Norköping, Linköping University, SE-601 74 Norköping, Sweden.*

***** Corresponding author e-mail: esbro@ifm.liu.se

Abstract

We report the piezoelectric properties of ZnO nanowires (NWs) obtained by using a nanoindenter with a conductive boron-doped diamond tip. The direct piezoelectric effect was measured by performing nanoindentations under load control, and the generated piezoelectric voltage was characterized as a function of the applied loads in the range 0.2-6 mN. The converse piezoelectric effect was measured by applying a DC voltage to the sample while there was a low applied force to allow the tip being always in physical contact with the NWs.

Vertically aligned ZnO NWs were grown on inexpensive, flexible, and disposable paper substrate by a template-free low temperature aqueous chemical growth method. When using the nanoindenter to measure the direct piezoelectric effect, piezopotential values of up to 26 mV were generated. Corresponding measurement of the converse piezoelectric effect gave an effective piezoelectric coefficient d^{eff}_{33} *of ~9.2 pmV*$^{-1}$*. The ZnO NWs were also characterized by scanning electron microscopy, X-ray diffraction, and high-resolution transmission electron microscopy. The new nanoindentation approach provides a straightforward method to characterize piezoelectric material deposited on flexible and disposable substrates for the next generation of nanodevices.*

Keywords: ZnO, nanowires, piezoelectricity, direct piezoelectricity, converse piezoelectricity, nanoindentation

1. Introduction

Over the last decade, nanotechnology has changed and raised the level of human life style with the development of a wide range of nanoscaled applications. The functionality of these nanodevices is totally dependent on its powering, which is becoming a critical bottleneck. Intensive research has been focused on finding the best way to provide a very promising, efficient and cost-effective power source and make the possibility to widespread practical use of these nanodevices [1-2]. Numerous piezoelectric-based nanogenerators, such as ZnO, InN, and CdS nanowires have been already explored as possible sources for converting mechanical energy into power [3-4].

Zinc oxide (ZnO), a direct wide bandgap compound, is widely exploited and extensively used as a piezoelectric material because, comparing with similar II-VI tetrahedrally bonded wurtzite compound semiconductors like ZnS, CdS, and CdSe, it has at least double the piezoresponse [5-6]. The structure of ZnO consists of alternating planes in which each atom is tetrahedrally coordinated, with the O^{2-} and Zn^{2+} ions stacked alternatively along the c-axis, and the center of gravity of the charges is at the center of the tetrahedron where positive and negative charges cancel each other. The lack of center of symmetry combined with the large electromechanical coupling results in a strong piezoelectric response [3,7]. The piezoelectric properties of ZnO, extensively studied in theoretical [8-9] and experimental works [5,10], are exploited in a wide spectrum of applications like transducers, sensors, and actuators ([11-14] and references therein).

Zinc oxide presents various types of one dimensional (1D) nanostructures including nanowires (NWs), nanorods (NRs), nanobelts (NBs), and nanotubes, which can be synthesized under specific growth conditions, as has been recently reviewed by Wang [7] and Niederberger [15]. Theoretical calculations have shown that ZnO piezoelectricity in 1D nanostructures is preserved with a possibility of enhanced performance due to the free

boundary for volume expansion/contraction [7,16], with direct implications in the development of novel practical applications like flexible piezoelectric NRs strain sensors [17-18], piezoelectric NW FETs [19], and the use of ZnO NW arrays for the nanoscale conversion from mechanical to electric energy [1].

The techniques for piezoelectric characterization of thin films and nanostructured materials fall into two categories: measuring small surface displacements generated by an applied electric field (converse piezoelectricity), and measuring a charge or voltage generated by an applied force on the sample (direct piezoelectricity). The most common method for characterization of converse piezoelectricity in nanostructures usually involves the use of piezoresponse force microscopy (PFM) [16]. This method is based on the detection of the induced displacement (often in the picometer range) by a local electric field applied to a conductive tip in an atomic force microscope (AFM). PFM has been used to characterize 1D ZnO nanostructures like NWs [1], NBs [20], and NRs [10]. The measurement of direct piezoelectricity in nanostructures involves tensile loading or lateral bending of the material with simultaneous measurement of generated charge or electric potential. In the literature, the direct piezoelectric measurement of 1D ZnO nanostructures has only been presented in the context of piezoelectric nanogenerators [1, 21].

In this study, we report for the first time the use of a nanoindenter to measure direct and converse piezoelectricity of high-quality ZnO NWs grown on paper substrates. The microstructural and morphological properties of the NWs, measured by scanning electron microscopy, X-ray diffraction, and high-resolution transmission electron microscopy, are correlated to the piezoelectrical properties.

2. Experimental details

Clean-room paper (PUREImage™ from VWR) was ultrasonically cleaned with deionized (DI) water and dried with nitrogen. Poly (3,4-ethylenedioxythiophene)-polystyrene sulfonate acid (PEDOT:PSS) was spin coated on the paper substrate at a rate of 2100 rpm during 30 s. The substrate was subsequently baked at 100 °C for 5 min to form a uniform PEDOT:PSS film of about 60 nm thick [22] and a conductivity of 80 S/cm [23]. The ZnO NWs used in this experiment were synthesized by a simple, very economic and a template-free low temperature aqueous chemical growth (ACG) method, as described previously [21, 24]. A seed layer, which provides nucleation sites for the growth of ZnO NWs, was spin-coated four times onto the substrates at a rate of 2,200 rpm for 1 min. The seed layer was prepared by mixing zinc acetate dehydrate ($C_4H_6O_4Zn{\cdot}2H_2O$) in methanol to obtain a 0.01 M solution concentration. This solution was then heated up to 60 ^{0}C. Another solution of KOH in methanol (0.03 M) was added to the first solution under continuous stirring, and the whole solution was kept at 60 °C for 2 h. After the spin-coating, the substrates were heated in air at a constant temperature of 80 °C for 20 min in order to solidify the seed layer. To grow the ZnO NWs, zinc nitrate hexahydrate [$Zn(NO_3)_2{\cdot}6H_2O$] (99.998%) and hexamethylenetetramine ($C_6H_{12}N_4$) (99.998%) were mixed with equal molar concentration in DI water and kept under continuous magnetic stirring for 30 min to get a uniform growth solution. The seeded substrates were then placed in the solution and were heated at 90 °C for 5 h. After the growth, the samples were rinsed with DI water to remove by excess salt on the surface, and then the samples were blown dry with nitrogen.

The surface morphology and dimensions of the resulting ZnO NWs were observed by scanning electron microscopy (SEM) in a Zeiss Leo 1550 instrument operating at 12 keV. The crystal structure and phase identification of the NRs were characterized by using X-ray diffraction (XRD) with Cu Kα radiation operating at 40 keV and 100 mA. The NWs were also

investigated by transmission electron microscopy (TEM) in a FEI Tecnai G2 TF20 UT with a field emission gun operated at 200 kV and a point resolution of 0.19 nm. ZnO NWs were scratched off the substrate followed by ultrasonication in ethanol in order to disperse them. Drops of the liquid containing ZnO NWs were deposited on standard carbon-coated grids.

Nanoindentation with *in-situ* electrical characterization was used to characterize the nanoscale electromechanical properties of the piezoelectric ZnO NWs. Testing was performed using a Triboindenter TI-950 (Hysitron), which was adapted to perform piezoelectrical measurements using a conductive boron-doped diamond Berkovich tip with a resistivity of ~3 Ω-cm. During all the piezoelectric measurements, the samples remained at constant room temperature.

3. Results and discussion

3.1 Microstructure and Morphology

Figure 1 show typical SEM images of ZnO nanowires grown by the ACG method on paper substrate. The ZnO NWs exhibit an apparent uniform distribution parallel to each other and predominately in a perpendicular orientation to the substrate. The approximate diameter of the NWs was about 150 ± 55 nm, while their length resulted 2300 ± 120 nm. The insets show that the NWs have a hexagonal cross-section.

Figure 2 is a typical XRD pattern of ZnO NWs, revealing that all the diffraction peaks can be indexed as the hexagonal wurtzite structured ZnO phase, consistent with the standard values for bulk hexagonal ZnO [6, 25]. No diffraction peaks of Zn or other impurities have been detected in the samples. The relatively enhanced intensity and sharp dominant peak at 34.40 degrees corresponding to the (002) peak indicates that the nanowires are highly c-axis oriented and normal to the paper substrate surface [26]. The small peak between the (101) and

(002) reflections can be related to a shift of the (002) peak probably due to stresses generated in a folded part of the paper substrate.

TEM analysis shows that the ZnO NWs have a single-crystalline structure and the axial direction is along the [0001] as shown in Figure 3 (a). The corresponding selected area electron diffraction (SAED) pattern in Figure 3(b) indicates that the ZnO NW has a single-crystal hexagonal wurtzite structure. Figure 3(c) presents a high-resolution TEM image taken from the top part of a ZnO NW. It can be clearly seen that the ZnO crystal lattices are well oriented with the lattice spacing of 0.52 nm, which corresponds to the distance of (0001) lattice planes, showing that the [0001] is the preferred growth direction for the ZnO NWs.

3.2 Converse Piezoelectric Effect

Converse piezoelectric tests were performed by nanoindentation testing using the configuration shown in Figure 4. The converse piezoelectric effect is measured by applying a DC voltage in the range 0 to -40 V while there is a low applied force to the sample of 50 μN, enough to allow the tip to be always in physical contact with the ZnO nanowires. This approach is similar to the method previously suggested by Rar *et al for* polycrystalline lead zirconate titanate (PZT) and $BaTiO_3$ piezoceramics [28], .ut in our case the applied voltage is DC instead of AC.

Figure 5 shows the load-displacement curve for the nanoindentation of NWs deposited on paper substrate. It is possible to observe that with a maximum load of 50 μN, the NW column is in stable equilibrium in the straight position, i.e., there is no buckling [29-30]. The experiment also shows that, during the time that the nanoindenter applies the maximum force, the curves present a creep of 35 nm. A similar creep behavior has been previously reported for ZnO nanorods [24].

Figure 6 shows the applied load and penetration depth as a function of time for the experimental data of Figure 5. The figure also indicates the elapsed time where a DC bias of -40V is applied to the substrate in order to make the piezo-characterization. We can observe how the NWs deform under the constant applied force of 50 μN, producing the creep (deformation) of the material which totals 35 nm after 45 s of applied constant force.

Figure 7 (a), a detailed view of Fig 6, shows the position of the tip as a function of time in the interval $10 \leq t \leq 40$ s, when a load of 50 μN is applied to the tip, and the bias is switched between 0 and -40 V every 10 s. We can see that there is a sharp change in the position when the bias is switched. Figure 7 (b) shows in more details the sharp change in the position of the tip of about $\Delta l \sim 37$ pm for the event around t = 15 s.

In order to evaluate the performance of any piezoelectric material clamped to a substrate, the most important parameter to calculate is the effective piezoelectric coefficient d^{eff}_{33}. In the case of NWs, this coefficient is directly related to the change of the longitudinal elongation Δl when the NWs are subject to a change in the applied voltage $\Delta \boldsymbol{V}$ in their c axis direction: $d^{eff}_{33} = \Delta l/\Delta \boldsymbol{V}$ [16]. From the result of Figure 7 (b) we can estimate $d^{eff}_{33} \sim$ 9.2 pm/V.

The converse piezoelectric effect d^{eff}_{33}, of technological use for the design of nanodevices, can be related to the "true" piezoelectric coefficient d_{33} of bulk material by the following relationship [16]:

$$d_{33} = d^{eff}_{33} (s_{11} + s_{12})/(s_{11}+s_{12}+s_{13}), \qquad (1)$$

where s_{11}, s_{12}, and s_{13} are the mechanical compliances of the piezoelectric NW. In our experiments we have not measured the compliance coefficients s_{ij} but we have found that d^{eff}_{33}, is very close to the accepted value for (0001) bulk ZnO of $d_{33} = 9.93$ pm/V [7].

The converse piezoelectric coefficient of some 1D ZnO nanostructures has been previously measured by PFM using AC voltages. For ZnO nanopillars with typical diameters

of ~300 nm, a piezoelectric constant of d^{eff}_{33} ~ 7.5 pm/V was obtained [31]. A similar study, for ZnO NRs with diameters in the range 150-500 nm and length of 400-600 nm, reported a variation of the piezoelectric constant from 0.4 to 9.5 pm/V [10]. The authors also observed that the variation of the d^{eff}_{33} was correlated to variations in the NRs resistivity: they concluded that a high conductivity quenches the piezoelectric response. PFM was also used to measure individual ZnO nanobelts in the (0001) surface, where d_{33} values in the range 3 to 26.7 pm/V were measured [20, 32]. To our knowledge, there is no data published about the piezoelectric constant d^{eff}_{33} of ZnO nanowires; the only reported values by PFM are generated voltages presented in the context of piezoelectric nanogenerators ([1, 21] and references therein).

3.4 Direct Piezoelectric Effect

Figure 8 shows the nanoindenter configuration used in our experiments. The direct piezoelectric effect was obtained by performing nanoindentations under load control with maximum load forces F_m ranging from 0.2 to 6 mN, while the generated piezoelectric voltage was measured as a function of the applied loads. This approach is similar to the method suggested by Koval *et al* for lead zirconate titanate thin films [1], but in their case the collected data were transient currents generated during the indentation.

The loading/unloading indentation test consisted of an "impulse force" with four parts (Figure 9): during the first 3 s the probe is in electric contact with the surface with an applied load of 2 μN; then the force over the probe increases linearly in 1 s to the maximum value F_m; in the third part the load decreases linearly in 1 s from F_m to 2 μN, and finally the probe rests over the sample during 3 s with an applied load of 2 μN to allow possible relaxation processes to occur. Ten indentations separated by a distance of ~50 μm were made in each sample.

The generated voltage measured as a function of the applied force with F_m = 1 mN is presented in Figure 10. It can be observed that the produced voltage is approximately linear with the applied force.

Figure 11 compares the measured voltage levels as a function of the maximum force F_m for NWs deposited on paper substrates. The figure demonstrates that the generated voltage has two linear zones with a change of slope at F_m ~ 1 mN. The "kink" in the curves at around 1 mN may be an indication of a threshold for plastic deformation of the NWs. The behavior suggests that the plastic deformation induced by the indentation does not result in voltage generation. The plastic deformation possibly originates from slip dislocations from the nano-columnar structures, while the elastic deformations relates to compression of the lattice and the resulting piezoelectric potential. Further work is required to investigate the nature of the plastic deformations and related piezoelectric properties of the ZnO nanowires.

4. Conclusions

The direct and converse piezoelectric properties of highly c-axis oriented ZnO nanowires grown normal to a paper substrate by low temperature ACG method were measured for the first time by a nanoindentation technique. The converse piezoelectric effect was measured by applying a DC voltage to the sample while there was a low (50 µN) applied force to the sample. The direct piezoelectric effect was measured by performing nano-indentations under load control, and the generated piezoelectric voltage was characterized as a function of the applied loads in the range 0.2-6 mN.

When the nanoindenter is used to measure the converse piezoelectric effect, the NWs grown on paper substrate show an effective piezoelectric coefficient d^{eff}_{33} ~ 9.2 pm/V. When the nanoindenter is used to measure the direct piezoelectric effect, piezopotential values of up to 26 mV were generated. It was also shown that at the higher loads the ZnO NWs generate

proportionally less voltage, presumably due to plastic deformation of the material which does not contribute to generated voltage. It is demonstrated that the new measurement approach provides a straightforward method to characterize piezoelectric material deposited on flexible and disposable substrates for the next generation of nanodevices.

5. Acknowledgements

EB and LS acknowledge the support from the Swedish Government Strategic Research Area Grant in Materials Science at Linköping University (SFO-Mat-LiU) on Advanced Functional Materials. MYS and MW acknowledge the Swedish Research Council. The authors also acknowledge Dr. Ijaz Hussain Asghar for the help in the preparation of samples.

References

[1] Z. L. Wang and J. Song, "Piezoelectric nanogenerators based on zinc oxide nanowire arrays," *Science,* vol. 312, no. 5771, pp. 243-246, 2006.

[2] A. Curtright, P. Bouwman, R. Wartena and K. Swider-Lyons, "Power sources for nanotechnology," *International Journal of Nanotechnology,* vol. 1, no. 1, pp. 226-239, 2004.

[3] U. Ozgur, Y. I. Alivov, C. Liu, A. Teke, M. A. Reshchikov, S. Dogan, V. Avrutin, S.-J. Cho and H. Morkoc, "A comprehensive review of ZnO materials and devices," *Journal of Applied Physics,* vol. 98, no. 4, pp. 041301-103, 2005.

[4] R. Que, Q. Shao, Q. Li, M. Shao, S. Cai, S. Wang and S.-T. Lee, "Flexible Nanogenerators Based on Graphene Oxide Films for Acoustic Energy Harvesting," *Angewandte Chemie,* vol. 124, no. 22, pp. 5514-5518, 2012.

[5] Z. Wang, "Piezipotential gated nanowire devices: Piezotronics and piezo-phototronics," *Nano Today,* vol. 5, pp. 540-552, 2010.

[6] J. Wang and M. Isshiki, "Wide-Bandgap II-VI Semiconductors: Growth and Properties," in *Springer Handbook of Electronic and Photonic Materials*, USA, Springer-Verlag, 2007, p. Ch. 16.

[7] Z. Wang, "Zinc oxide nanostructures: growth, properties and applications," *Journal of Physics:*

Condensed Matter, vol. 16, pp. R829-R858, 2004.

[8] C. Li, W. Guo, Y. Kong and H. Gao, "First-principles study of the dependence of ground-state structural properties on the dimensionality and size of ZnO nanostructures," *Physical Review B,* vol. 76, no. 3, p. 035322, 2007.

[9] S. Dai, M. Dunn and H. Park, "Piezoelectric constants for ZnO calculated using classical polarizable core–shell potentials," *Nanotechnology,* vol. 21, no. 44, p. 445707, 2010.

[10] D. Scrymgeour and J. Hsu, "Correlated Piezoelectric and Electrical Properties in Individual ZnO Nanorods," *Nano Letters,* vol. 8, no. 8, pp. 2204-2209, 2008.

[11] U. Özgür, D. Hofstetter and H. Morkoç, "ZnO Devices and Applications: A Review of Current Status and Future Prospects," *Proceedings of the IEEE,* vol. 98, no. 7, pp. 1255 - 1268, 2010.

[12] A. Wei, L. Pan and W. Huang, "Recent progress in the ZnO nanostructure-based sensors," *Materials Science and Engineering B,* vol. 176, no. 18, pp. 1409-1421, 2011.

[13] S. Arya, S. Saha, J. Ramirez-Vick, V. Gupta, S. Bhansali and S. Singh, "Recent advances in ZnO nanostructures and thin films for biosensor applications: Review," *Analytica Chimica Acta,* vol. 737, no. 8, pp. 1-21, 2012.

[14] S.-J. Chen, Y. Choe, L. Baumgartel, A. Lin and E. Kim, "Edge-released, piezoelectric MEMS acoustic transducers in array configuration," *Journal of Micromechanics and Microengineering,* vol. 222, p. 025005, 2012.

[15] M. Niederberger, "Nonaqueous Sol–Gel Routes to Metal Oxide Nanoparticles," *Accounts of Chemical Research,* vol. 40, no. 9, p. 793–800, 2007.

[16] H. Espinosa, R. Bernal and M. Minary-Jolandan, "A Review of Mechanical and Electromechanical Properties of Piezoelectric Nanowires," *Advanced Materials,* vol. 24, no. 34, p. 4656–4675, 2012.

[17] J. Zhou, Y. Gu, P. Fei, W. Mai, Y. Gao, R. Yang, G. Bao and Z. Wang, "Flexible Piezotronic Strain Sensor," *Nano Letters,* vol. 8, no. 9, p. 3035–3040, 2008.

[18] H. Gullapalli, V. Vemuru, A. Kumar, A. Botello-Mendez, R. Vajtai, M. Terrones, S. Nagarajaiah and P. Ajayan, "Flexible Piezoelectric ZnO–Paper Nanocomposite Strain Sensor," *Small,* vol. 6, no. 15, p. 1641–1646, 2010.

[19] Y. Park, H. Choi, J.-H. Kim, J. Kim and Y.-B. Hahn, "High performance field-effect transistors fabricated with laterally grown ZnO nanorods in solution," *Nanotechnology,* vol. 22, p. 185310, 2011.

[20] M.-H. Zhao, Z.-L. Wang and S.-X. Mao, "Piezoelectric Characterization of Individual Zinc Oxide Nanobelt Probed by Piezoresponse Force Microscope," *Nano Letters,* vol. 4, no. 4, p. 587–

590, 2004.

[21]M. Y. Soomro, I. Hussain, N. Bano, O. Nur and M. Willander, "Piezoelectric power generation from zinc oxide nanowires grown on paper substrate," *Physica Status Solidi (RRL) - Rapid Research Letters,* vol. 6, no. 2, pp. 80-82, 2012.

[22]A. Wadeasa, O. Nur and M. Willander, "The effect of the interlayer design on the electroluminescence and electrical properties of n-ZnO nanorod/p-type blended polymer hybrid light emitting diodes," *Nanotechnology,* vol. 20, p. 065710, 2009.

[23]X. X. Crispin, F. L. E. Jakobsson, A. Crispin, P. C. M. Grim, P. Andersson, A. Volodin, C. van Haesendonck, M. Van der Auweraer, W. Salaneck and M. Berggren, "The Origin of the High Conductivity of Poly(3,4-ethylenedioxythiophene)−Poly(styrenesulfonate) (PEDOT−PSS) Plastic Electrodes," *Chemistry of Materials,* vol. 18, no. 8, p. 4354–4360, 2006.

[24]M. Soomro, I. Hussain, N. Bano, E. Broitman, .. O. Nur and M. Willander, "Nanoscale elastic modulus of single horizontal ZnO nanorod using nanoindentation experiment," *Nanoscale Research Letters,* vol. 7, p. 146, 2012.

[25]M. Soomro, I. Hussain, N. Bano, J. Lu, L. Hultman, .. O. Nur and M. Willander, "Growth, Structural and Optical Characterization of ZnO Nanotubes on Disposable-Flexible Paper Substrates by Low-Temperature Chemical Method," *Journal of nanotechnology,* p. 251863, 2012.

[26]M. Wang, C. Ye, Y. Zhang, H.-X. Wang, X.-Y. Zeng and L.-D. Zhang, "Seed-layer controlled synthesis of well-aligned ZnO nanowire arrays via a low temperature aqueous solution method," *Journal of Materials Science: Materials in Electronics,* vol. 19, no. 3, pp. 211-216, 2008.

[27]L. B. Freund and S. Suresh, Thin Film Materials, New York: Cambridge University Press, 2003.

[28]A. Rar, G. Pharr, W. Oliver, E. Karapetian and S. Kalinin, "Piezoelectric Nanoindentation," *Journal of Materials Research,* vol. 21, pp. 552-556, 2006.

[29]M. Riaz, O. Nur, M. Willander and P. Klason, "Buckling of ZnO nanowires under uniaxial compression," *Applied Physics Letters,* vol. 92, no. 10, pp. 103118 - 103118-3, 2008.

[30]M. Riaz, A. Fulati, L. L. Yang, O. Nur, M. Willander and P. Klason, "Bending flexibility, kinking, and buckling characterization of ZnO nanorods/nanowires grown on different substrates by high and low temperature methods," *Journal of Applied Physics,* vol. 104, no. 10, pp. 104306 - 104306-8, 2008.

[31]H. Fan, W. Lee, R. Hauschild, M. Alexe, G. Le Rhun, R. Scholz, A. Dadgar, K. Nielsch, H. Kalt, A. Krost, Z. M. and U. Gösele, "Template-Assisted Large-Scale Ordered Arrays of ZnO Pillars for Optical and Piezoelectric Applications," *Small,* vol. 2, no. 4, pp. 561-568, 2006.

[32]M.-H. Zhao, "Nanomechanical and Electromechanical Characterization of Zinc Oxide

Nanobelt Using Atomic Force Microscopy," PhD Thesis University of Pittsburgh, Pittsburgh, 2004.

[33]V. Koval, M. Reece and A. Bushby, "Ferroelectric/ferroelastic behavior and piezoelectric response of lead zirconate titanate thin films under nanoindentation," *Journal of Applied Physics,* vol. 97, p. 074301, 2005.

Legend to Figures

Figure 1: SEM image of ZnO nanowires grown on paper substrate. The inset shows a high magnification image of a single ZnO nanowire with well-defined hexagonal end planes

Figure 2: X-ray diffraction pattern of ZnO NWs grown on paper substrat.

Figure 3: (a) TEM image of a single ZnO nanowire; (b) SAED pattern of a single nanowire; (c): HRTEM image of the ZnO nanowire.

Figure 4: Schematic drawing of the experimental setup for the measurement of the converse piezoelectric effect by nanoindentation.

Figure 5: Load-displacement curve for the nanoindentation of a NW deposited on paper substrate. The probe was a boron-doped diamond Berkovich tip, and the experiments were done in the load-control mode.

Figure 6: Applied load and penetration depth as a function of elapsed time during the nanoindentation of ZnO NWs grown on paper substrate. The elapsed time where a DC -40V bias is applied has been indicated as a center line.

Figure 7: Detailed views of the penetration depth as a function of elapsed time t during the nanoindentation of NWs deposited on paper substrate (Figure 6) for (a) $10 < t < 40$ sec, and (b) $14 < t < 16$ seconds.

Figure 8: Schematic drawing of the experimental setup for the measurement of the direct piezoelectric effect by nanoindentation.

Figure 9: Loading/unloading indentation curve used to measure the direct piezoelectric effect. The maximum load force F_m range was fixed between 0.2 and 6 mN.

Figure 10: Applied load and corresponding generated piezoelectric voltage as a function of the time for NWs grown on paper substrate. The maximum load force is 1 mN.

Figure 11: Generated piezo-voltage as a function of maximum applied load for NWs grown on (a) paper substrate. The dotted lines are for guiding the eyes only.

Figure 1

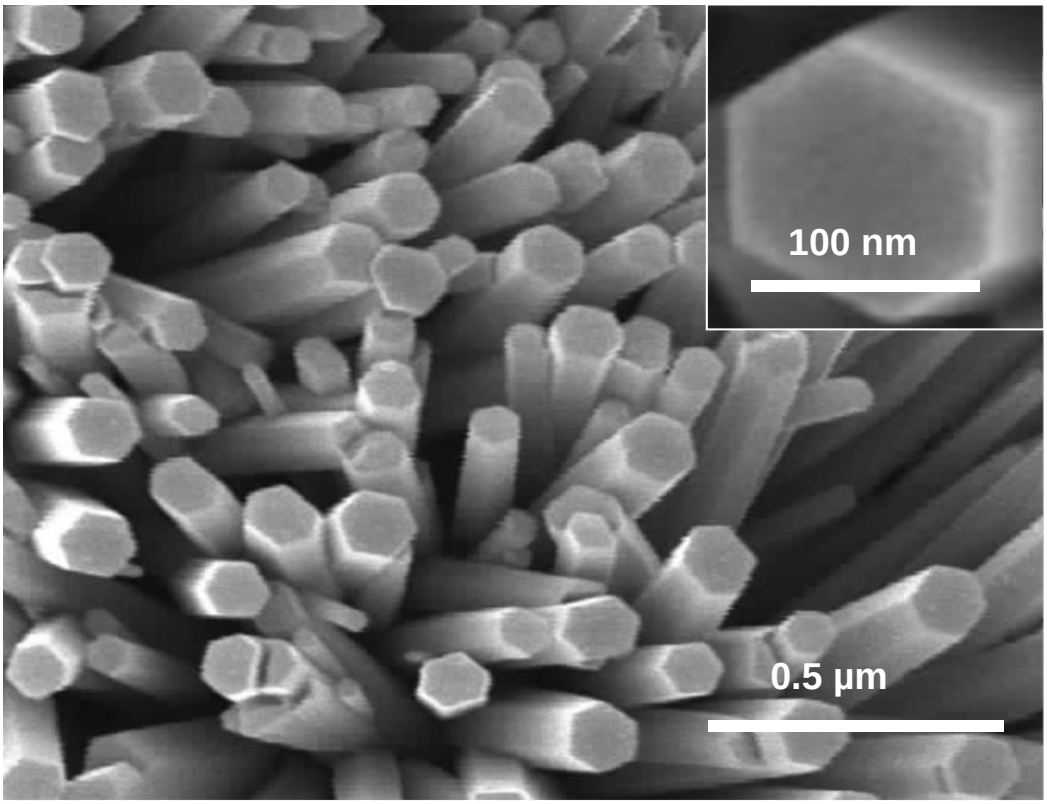

Figure 1: SEM image of ZnO nanowires grown on paper substrate. The inset shows a high magnification image of a single ZnO nanowire with well-defined hexagonal end planes

Figure 2

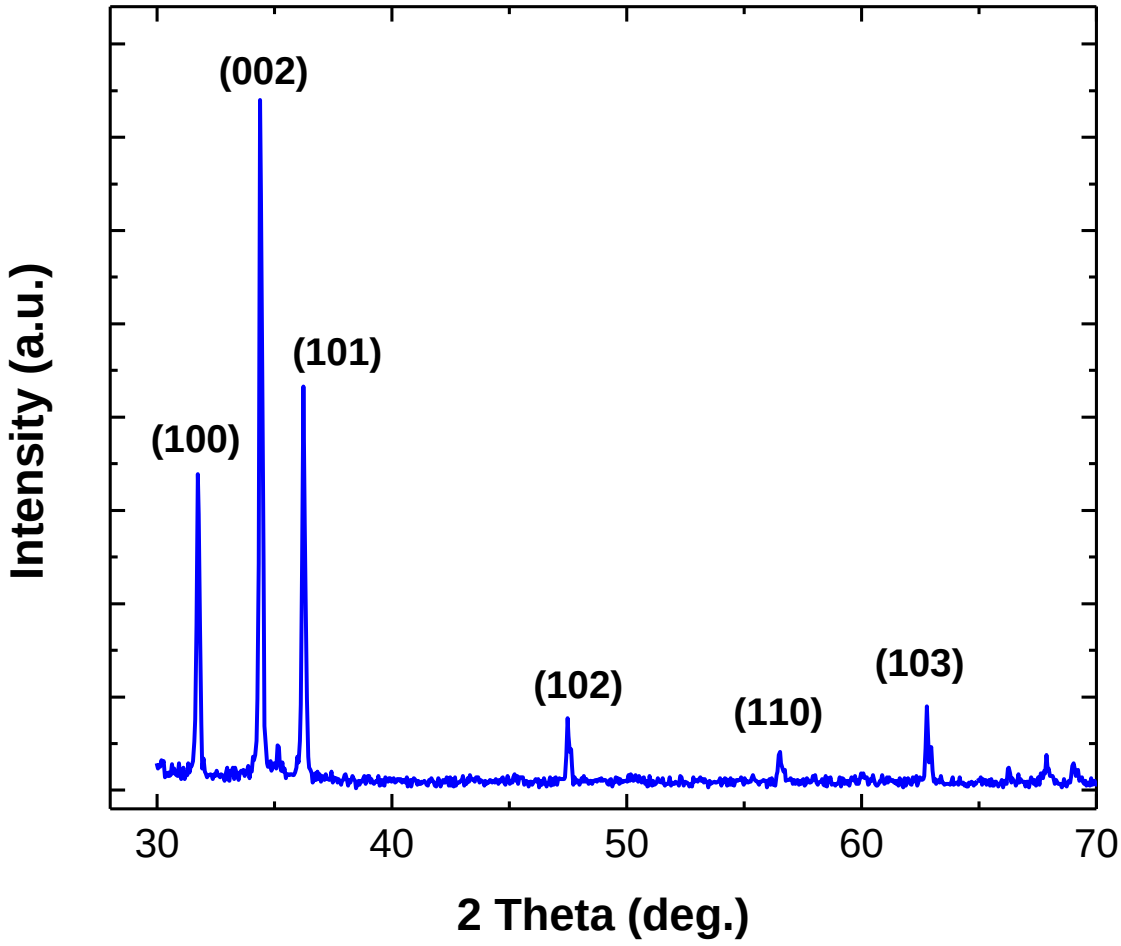

Figure 2: X-ray diffraction pattern of ZnO NWs grown on paper substrate.

Figure 3

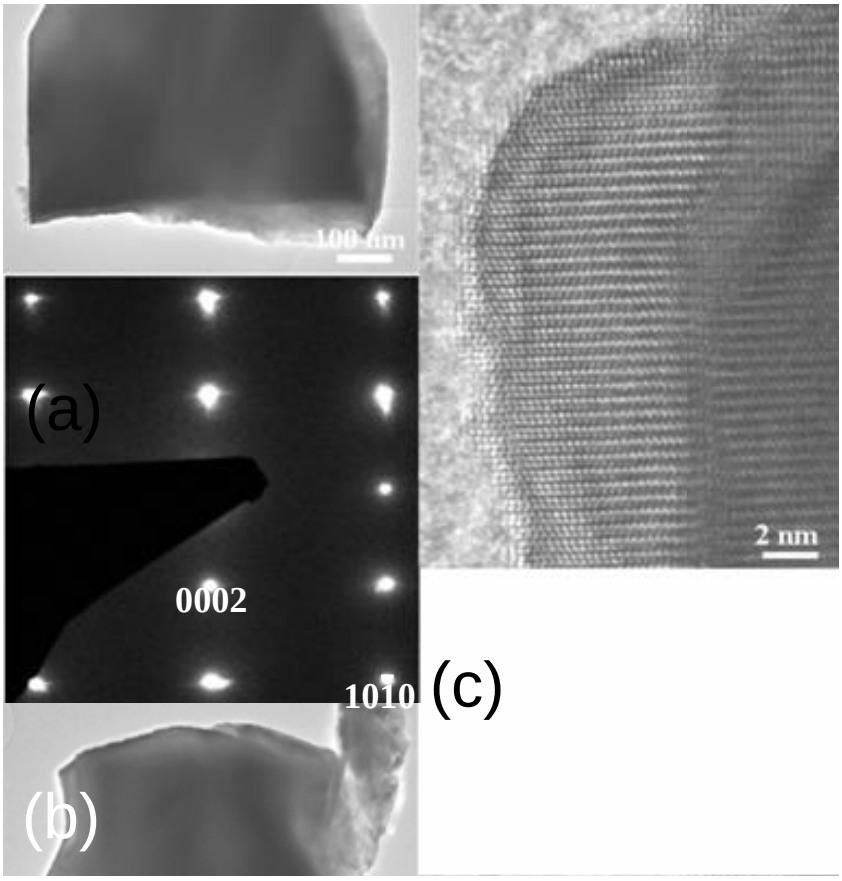

Figure 3: (a) TEM image of a single ZnO nanowire; (b) SAED pattern of a single nanowire; (c): HRTEM image of the ZnO nanowire.

Figure 4

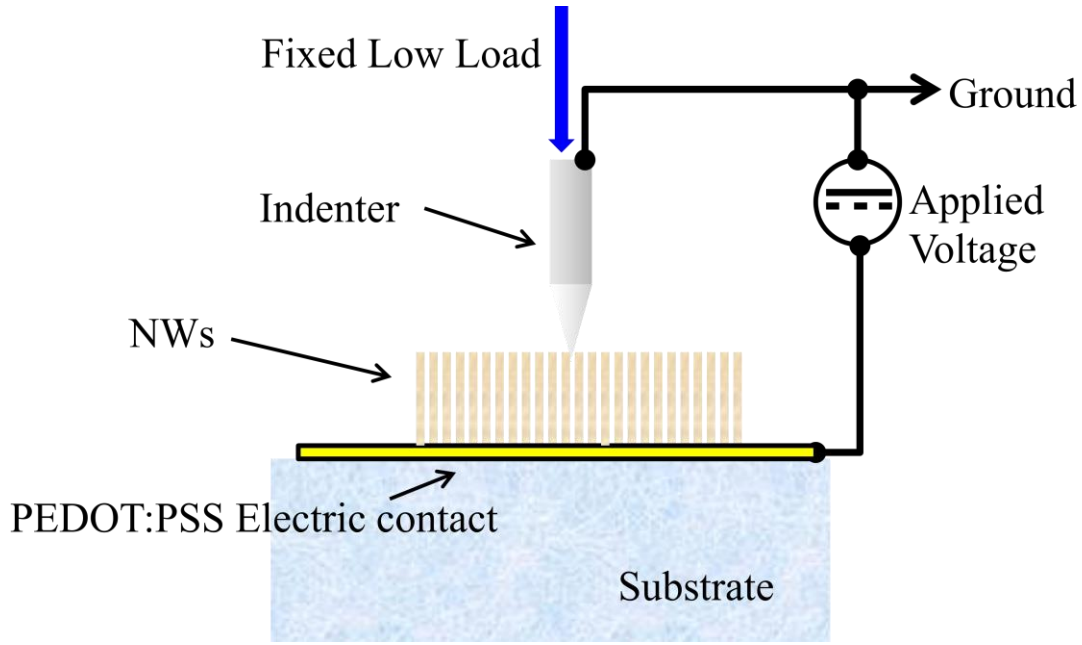

Figure 4: Schematic drawing of the experimental setup for the measurement of the converse piezoelectric effect by nanoindentation.

Figure 5

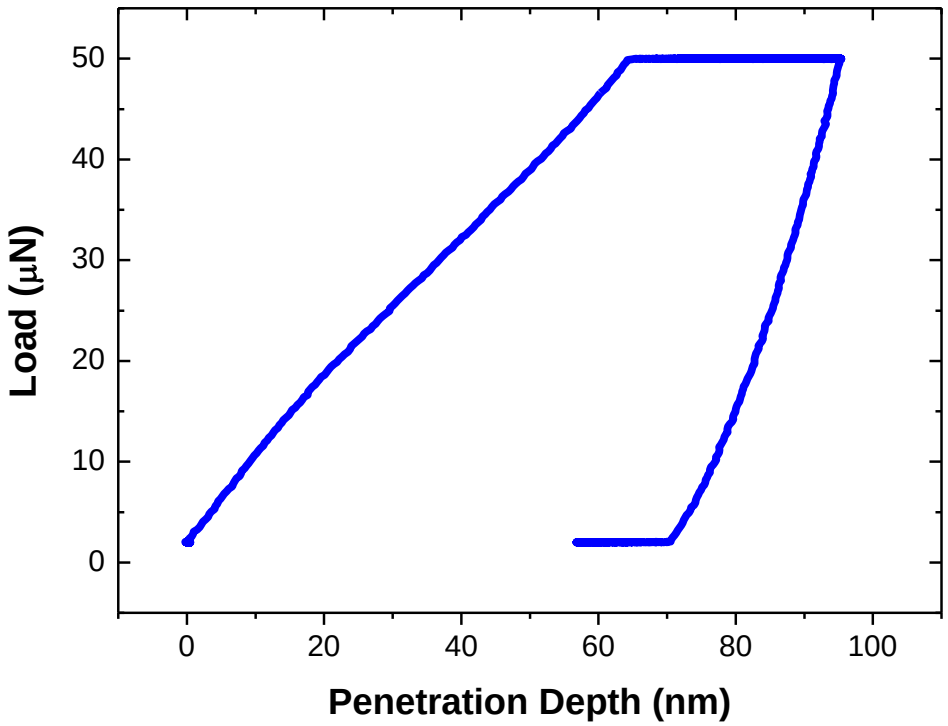

Figure 5: Load-displacement curve for the nanoindentation of a NW deposited on paper substrate. The probe was a boron-doped diamond Berkovich tip, and the experiments were done in the load-control mode.

Figure 6

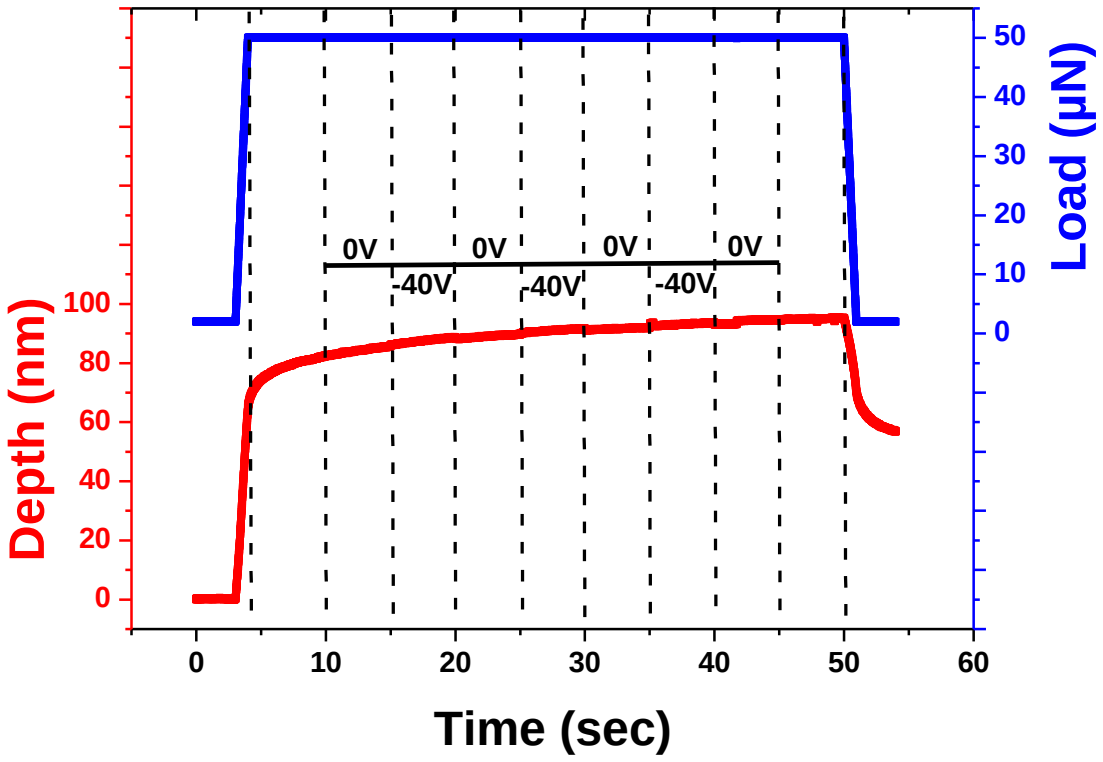

Figure 6: Applied load and penetration depth as a function of elapsed time during the nanoindentation of ZnO NWs grown on paper substrate. The elapsed time where a DC -40V bias is applied has been indicated as a center line.

Figure 7

Figure 7 (a)

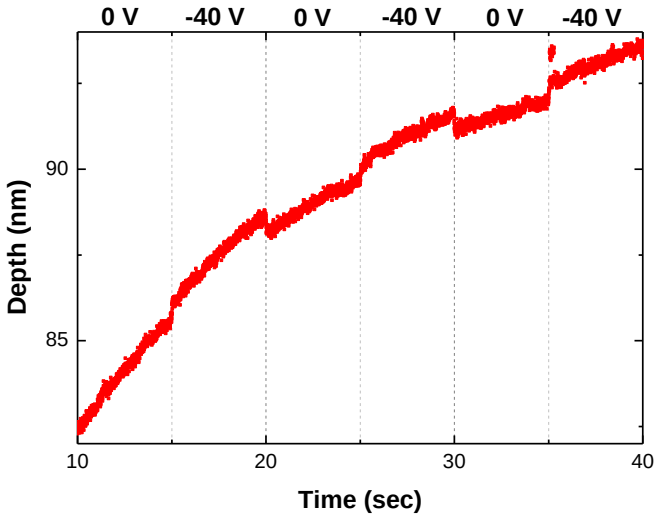

Figure 7 (b)

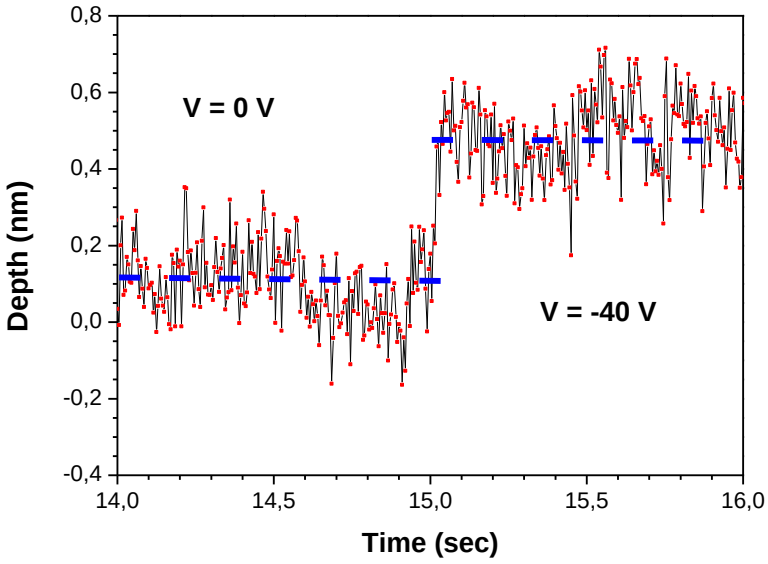

Figure 7: Detailed views of the penetration depth as a function of elapsed time t during the nanoindentation of NWs deposited on paper substrate (Figure 6) for (a) 10 < t < 40 sec, and (b) 14 < t < 16 seconds.

Figure 8

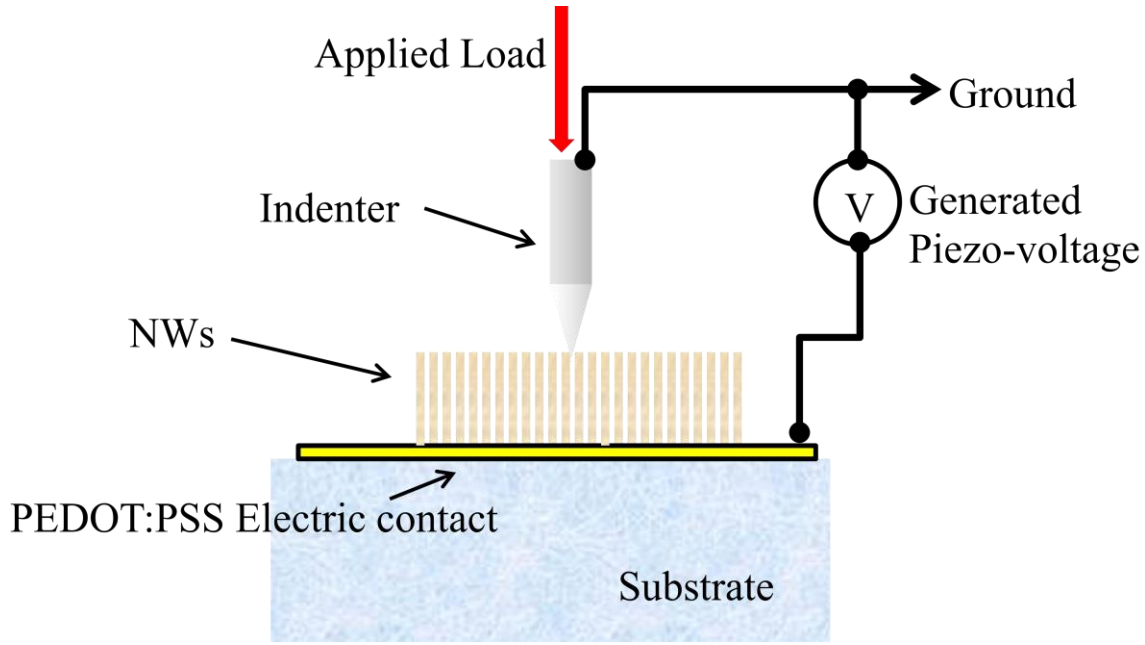

Figure 8: *Schematic drawing of the experimental setup for the measurement of the direct piezoelectric effect by nanoindentation.*

Figure 9

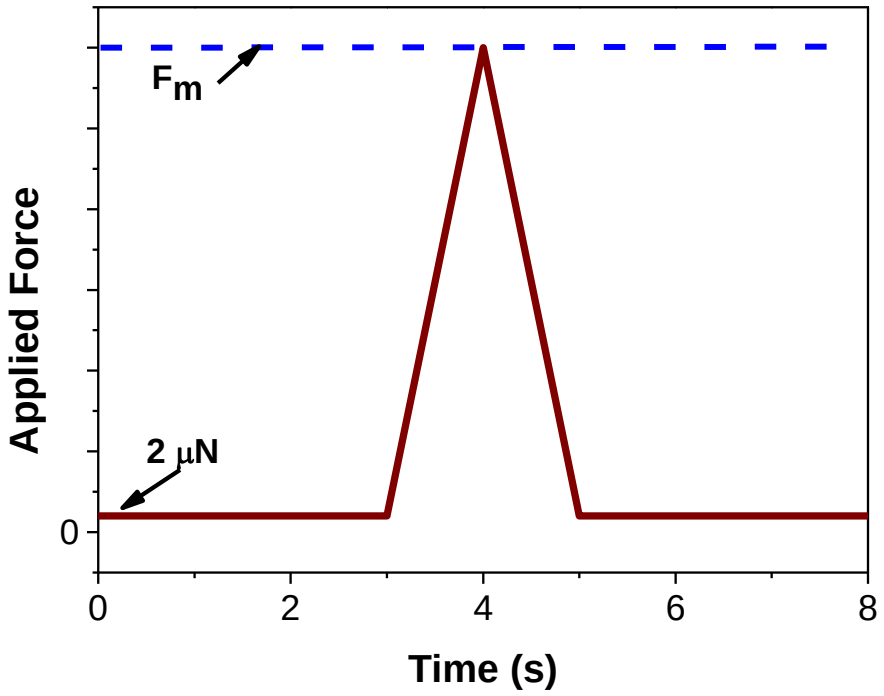

Figure 9: Loading/unloading indentation curve used to measure the direct piezoelectric effect. The maximum load force F_m range was fixed between 0.2 and 6 mN.

Figure 10

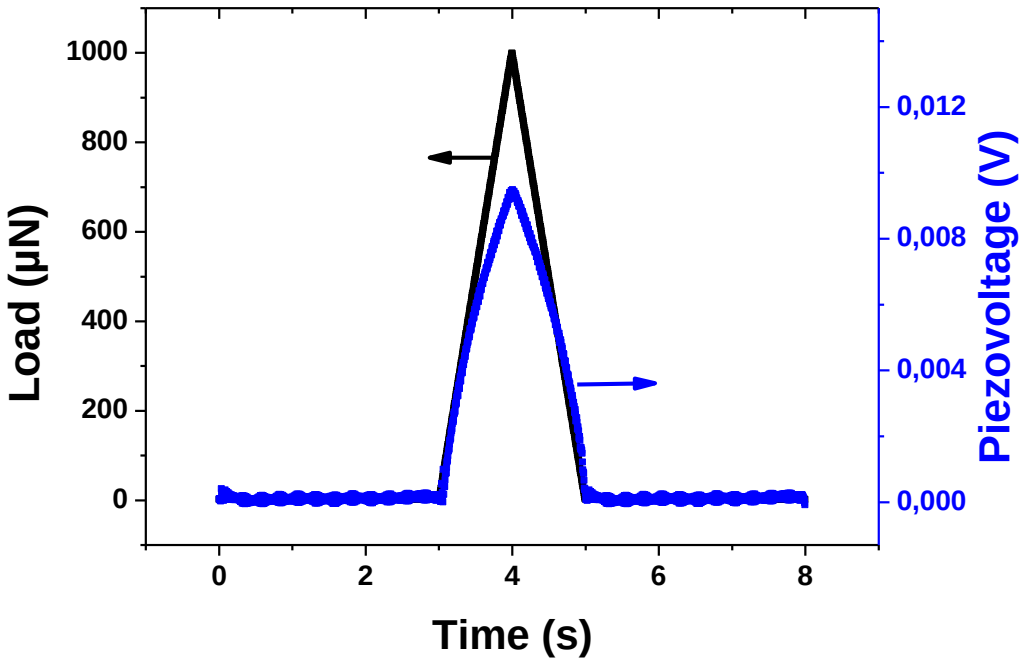

Figure 10: Applied load and corresponding generated piezoelectric voltage as a function of the time for NWs grown on paper substrate. The maximum load force is 1 mN.

Figure 11

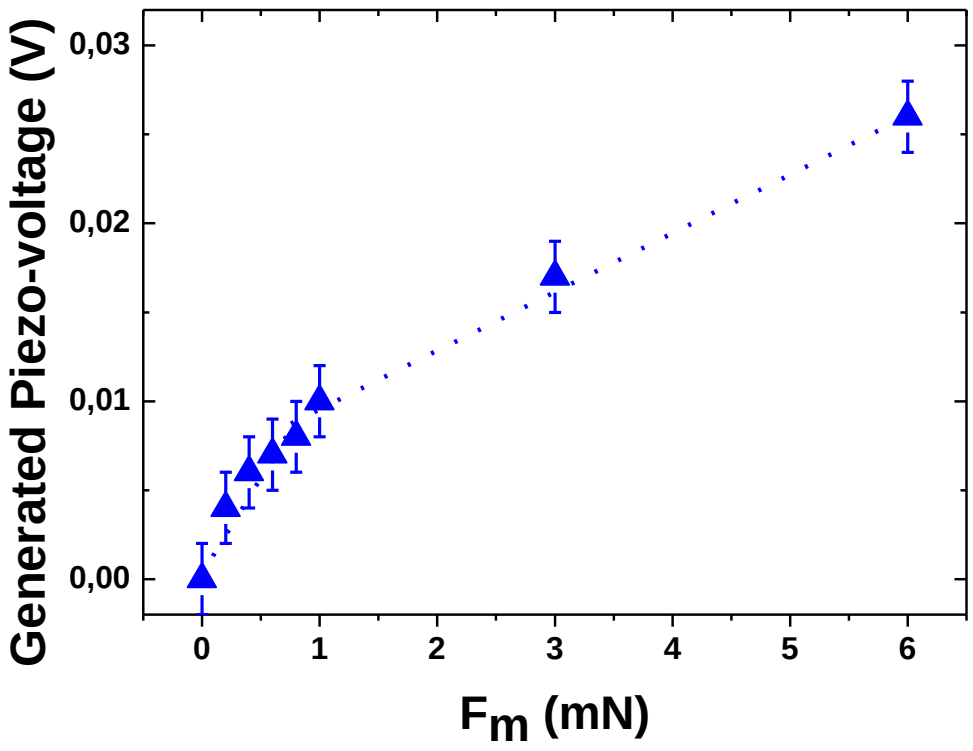

Figure 11: Generated piezo-voltage as a function of maximum applied load for NWs grown on (a) paper substrate. The dotted lines are for guiding the eyes only.